

Electronic Supplementary Information

Formation of Bilayer Clathrate Hydrates

Wen-Hui Zhao,^{a,#} Jaeil Bai,^{b,#} Lu Wang,^a Lan-Feng Yuan,^{*a} Jinlong Yang,^a Joseph
S. Francisco^b and Xiao Cheng Zeng^{*a,b}

^aHefei National Laboratory for Physical Sciences at Microscale, Department of
Chemical Physics and Collaborative Innovation Center of Chemistry for
Energy Materials, University of Science and Technology of China, Hefei,
Anhui 230026, China

^bDepartment of Chemistry, University of Nebraska-Lincoln, Lincoln, Nebraska
68588, USA

*Emails: *xzeng1@unl.edu; yuanlf@ustc.edu.cn*

#Both authors contribute equally to this work.

A. MD simulation of formation of the BL ethane hydrates

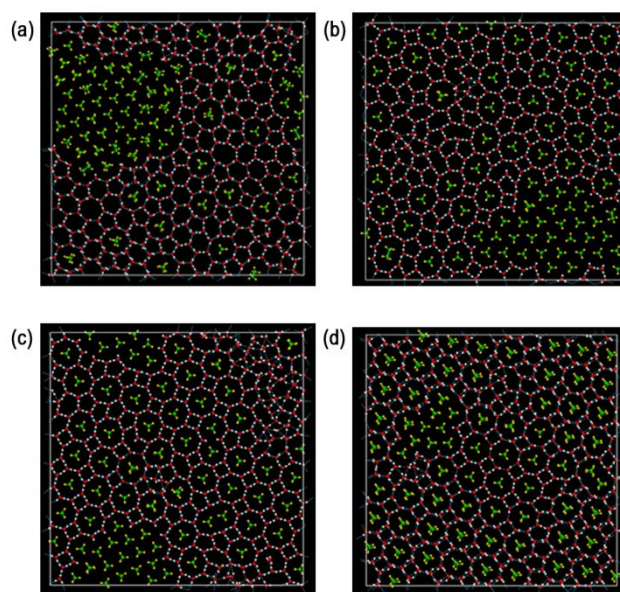


Figure S1. The inherent structures of BL solid of mixture of water and ethane, originally obtained from MD simulations at $P_L =$ (a) 200 MPa ($T = 210$ K), (b) 500 MPa ($T = 260$ K), (c) 800 MPa ($T = 320$ K), and (d) 1 GPa ($T = 350$ K), respectively.

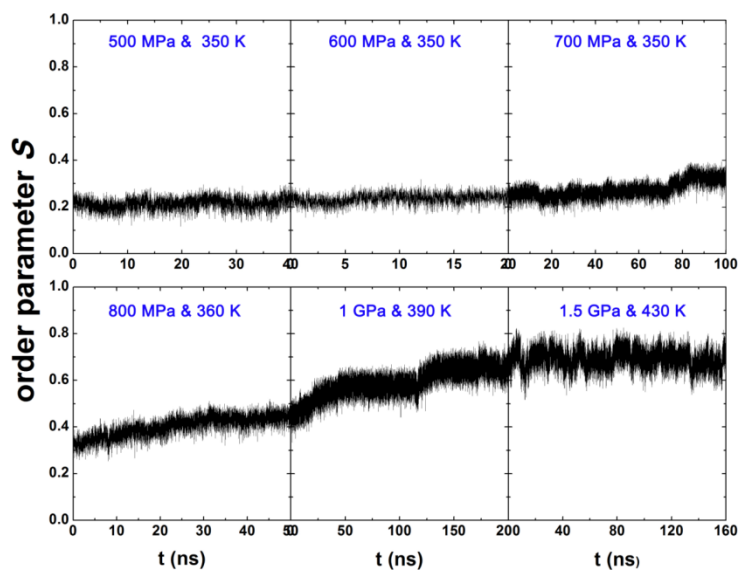


Figure S2. The order parameters S for describing growth of the BL ethane hydrate crystal from a three-phase coexisting structure.

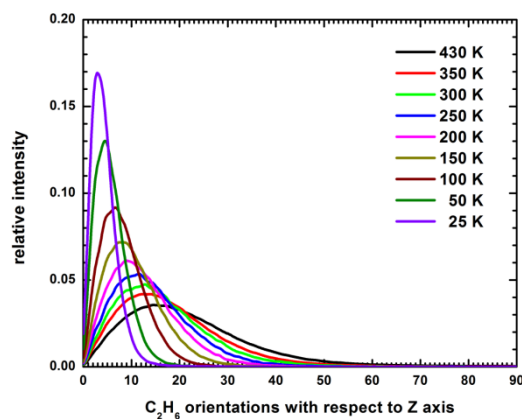


Figure S3. The ethane molecule orientation with respect to z -axis in the BL-clathrate hydrate at various temperatures. As temperature decreases majority of ethane molecules in the hydrate are aligned vertically (~ 3 degree at 25 K).

B. MD simulation of formation of the BL ethene and allene hydrates

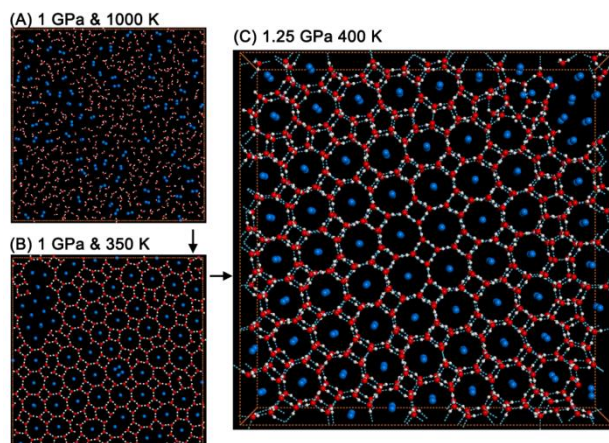


Figure S4. Thermodynamic path designed in an MD simulation to grow the BL ethene hydrate crystal. To increase the number of ethene molecules dissolved in the water, we first equilibrate the binary fluid mixture of water and ethene at 1000 K and 1 GPa (A). Then, the temperature is quenched to 350 K. After 100 ns equilibration, a BL amorphous ethene hydrate is obtained (B). In the amorphous hydrate, except a small domain of dense ethene bubble, most ethene molecules are trapped in BL-octagonal cages (including a few in BL-heptagonal cages as well) which are connected by BL-polygons (BL-pentagons and BL-tetragons in particular). Double occupancy, *i.e.*, two ethane molecules being trapped in a BL-decagon cage, is also observed. Next, the temperature is raised instantly to 380 K and kept for 100 ns, followed by an increase of temperature to 400 K and pressure to 1.5 GPa for another 100 ns. Lastly, the pressure is lowered to 1.25 GPa for 100 ns. Although a small domain of phase-separated ethene fluid and two chains of BL-pentagon defects remain within the BL hydrate, we can see that the perfect BL ethene hydrate is similar to the structure of the BL ice framework with the Archimedean $4 \cdot 8^2$ (square-octagon) pattern. The orientation of ethene molecules allows us to use the order parameter S to quantitatively describe nucleation of water cages (Figure S5).

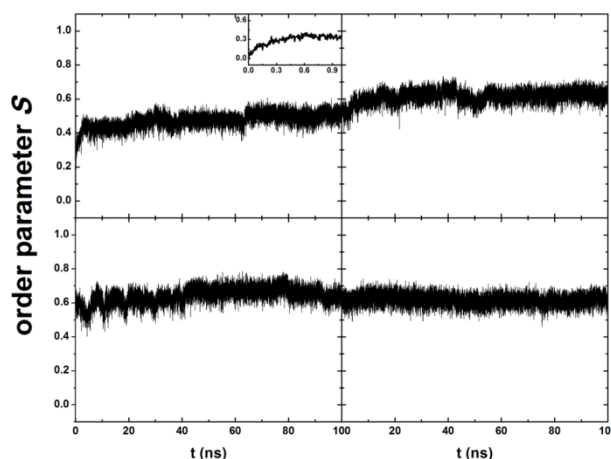


Figure S5. The order parameters S for describing growth of the BL ethene hydrate crystal from the mixture at 1000 K and 1 GPa. The inset shows most ethane molecules are separately trapped inside water cages within 1 ns of MD simulation. Hence, high-temperature initial structure can promote nucleation of water cages because more guest molecules can be dissolved in the water at high temperature.

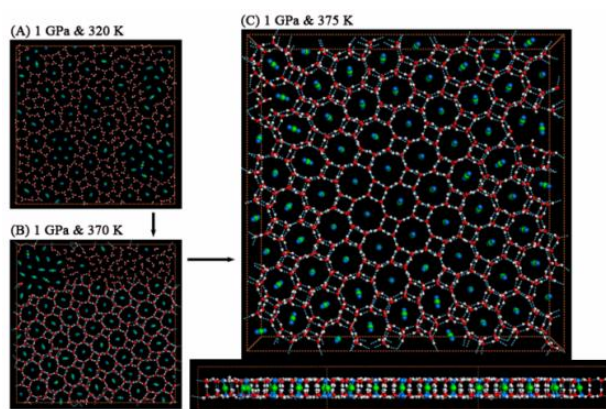


Figure S6. Thermodynamic path designed for an MD simulation of growth of the BL allene (C_3H_4) hydrate crystal. Starting from a mixture fluid equilibrated at 1000 K and 1 GPa, the system is quenched instantly to 320 K and kept for 100 ns (A), leading to a mixture structure in which many allene molecules are separately trapped in BL-octagonal cages and a few allene molecules form a dense allene bubble. Next, the octagon-square domains grow gradually to form a three-phase coexisting structure (B) upon repeated heating/annealing, compressing/decompressing ((340 K, 1.5 GPa) \rightarrow (360 K, 1.5 GPa) \rightarrow (360 K, 1.25 GPa) \rightarrow (360 K, 1 GPa) \rightarrow (355 K, 1.25 GPa) \rightarrow (360 K, 1.25 GPa) \rightarrow (365 K, 1.25 GPa) \rightarrow (370 K, 1.5 GPa) \rightarrow (380 K, 1.5 GPa) \rightarrow (390 K, 1.5 GPa) \rightarrow (400 K, 1.5 GPa) \rightarrow (380 K, 1.25 GPa) \rightarrow (370 K, 1 GPa)). Finally, a very long MD simulation (1 μ s) is performed at 1 GPa and 375 K to achieve a near-perfect BL allene hydrate crystal. (C) A top view and side view of the inherent structure of a near-perfect BL allene hydrate crystal, obtained from the MD simulation at 1 GPa and 375 K. Although the size of allene is larger than ethane, those allene molecules separately trapped inside the BL-octagonal cages are also perpendicular to the confining walls.

C. MD simulation of formation of the BL CO₂ amorphous hydrate

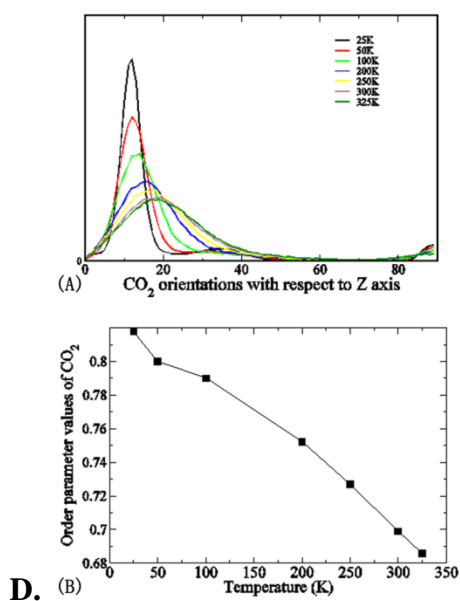


Figure S7. (A) CO₂ molecule orientation with respect to *z*-axis, and (B) the order parameter *S* of CO₂ versus temperature for the BL amorphous hydrate.

D. BL water and H₂S structure

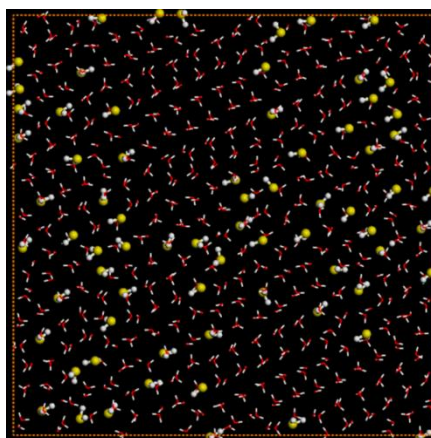


Figure S8. The inherent structure of BL mixture of water and H₂S (at 250 K and 1 GPa). The yellow spheres represent sulfur atoms. The structure resembles the BL-rhombic ice, except some defects such that water molecules are replaced by H₂S molecules, a feature similar to that of BL mixture of water and NH₃.

E. A structure of BL methane clathrate III

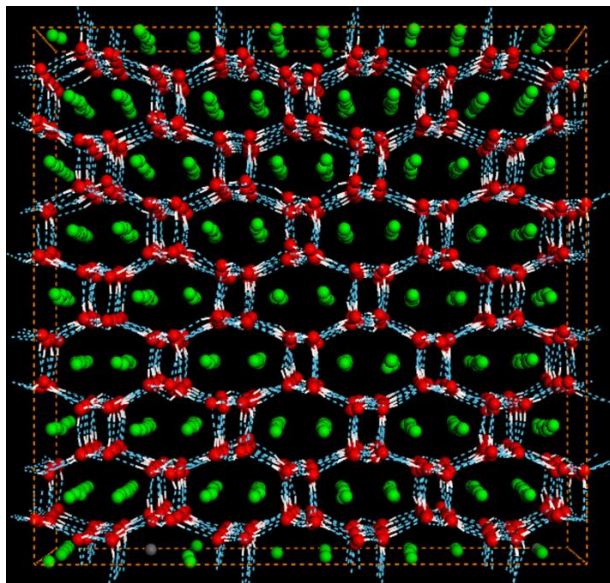


Figure S9. A snapshot of the methane clathrate III (at 3 GPa and 300 K).

F. Independent MD simulations with TIP4P water model.

Using the TIP4P water model, we also perform a series of independent MD simulations with the same systems to study the formation of the BL-clathrate for ethane, CO₂, H₂, or NH₃ molecules as guests. Spontaneous formation of these BL clathrate hydrates is also observed. Figure S10 shows the inherent structures of the four BL clathrate hydrates in which some defects are formed. We expect that near-perfect hydrates similar to those obtained using TIP5P water model can be also obtained *via* the multistep nucleation and growth.

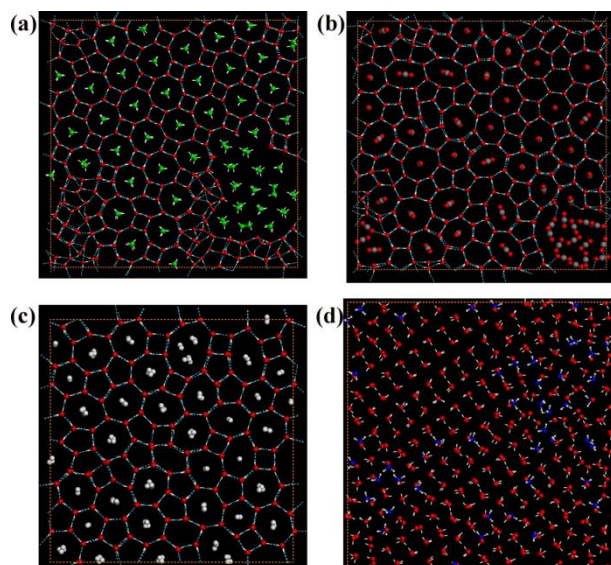


Figure S10. The inherent structures of less perfect BL clathrate hydrates for (a) ethane at 500 MPa and 330 K, (b) CO₂ at 500 MPa and 250 K, (c) H₂ at 1 GPa and 290 K, and (d) NH₃ at 1.5 GPa and 240 K, respectively.

G. Structural optimization of BL-octagon-tetragon and BL-hexagon hydrates using density-functional theory methods

Density functional theory (DFT) optimizations were performed by using QUICKSTEP,^{S1} a part of the CP2K package, to confirm structures of the BL hydrates observed in the classical MD simulations. The ion-valence electron interactions are represented by norm-conserving pseudopotentials developed by Goedecker and coworkers,^{S2,S3} and the charge density cutoff of 280 Ry is used for the auxiliary plane-wave basis set. The HCTH120 exchange-correlation functional^{S4} is selected. Kohn–Sham orbitals are expanded into a triple-zeta valence basis set augmented with two sets of *d*-type or *p*-type polarization functions (TZV2P). A strict convergence criterion is chosen for the electronic gradient 1×10^{-7} eV with the orbital transformation method. Convergence criterion for the maximum force was set to 0.01 eV/Å. Since the BL structures are quasi-two-dimensional, a tetragonal supercell is adopted for BL-octagon-tetragon ice with the lattice parameters *a* and *c*, and hexagonal supercell is adopted for BL-hexagon and BL-rhombic ices with the lattice parameters *a* and *c*. The *z*-direction is chosen to be the normal direction to the bilayer

surface. The lattice c is set to be 20 Å and fixed, while lattice a can be relaxed to achieve the lowest total energy.

The geometry optimization confirms that free-standing BL-octagon-tetragon and BL-hexagon ices, as shown in Figure S11, have the same structural features as those from the classical MD simulations, although the BL-octagon-tetragon ice is metastable up to 200 K whereas the BL-hexagon ice is the thermodynamically stable phase.^{S5} When the methane, ethane, ethene, or allene molecules are trapped in the center of the BL-octagonal cages, the BL-octagon-tetragon structures are stable (Fig. S11b; the figures for methane, ethene, and allene molecules are not shown as they are very similar to that for ethane molecule). The lattice a is slightly expanded compared to that of the guest-free BL-octagon-tetragon ice. The BL-hexagonal H₂ hydrate is also stable when the H₂ molecules are trapped in the center of the BL-hexagonal cages with the lattice a slightly expanded (Fig. S11d).

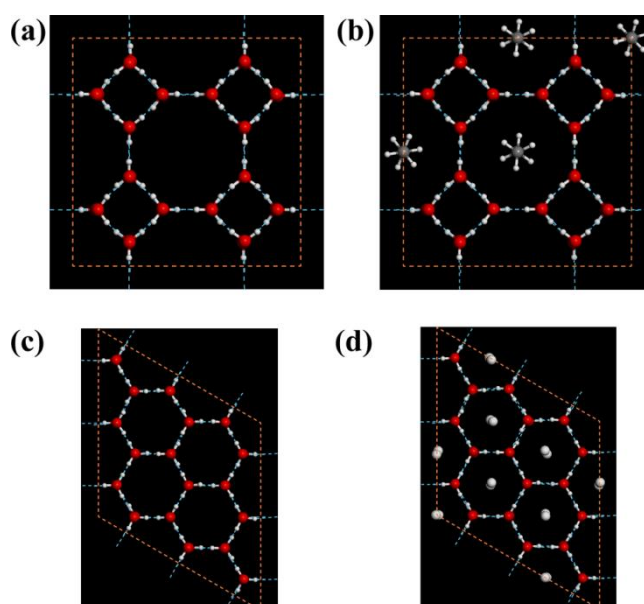


Figure S11. The DFT optimized structures of BL-octagon-tetragon (a) guest-free, (b) ethane hydrate, and BL-hexagon (f) guest-free (g) H₂ hydrate.

Table S1. The Lennard-Jones and Coulombic potential parameters for H₂O, C₂H₆, C₂H₄, C₃H₄, H₂, CO₂, NH₃ and H₂S.

		σ_i (nm)	ε_i (kJ/mol)	q (e)	σ_{iw} (nm)	ε_{iw} (kJ/mol)
H ₂ O ^{S6,S7}	O	0.312	0.66944	0.0	0.25	1.25
	H	0.0	0.0	0.241	0.0	0.0
	Site (1, 2)	0.0	0.0	-0.241	0.0	0.0
C ₂ H ₆ ^{S8}	CH ₃	0.3775	0.866088	0.0	0.275	1.89
C ₂ H ₄ ^{S8}	CH ₂	0.385	0.58576	0.0	0.278	1.60
C ₃ H ₄ ^{S8}	CH ₂	0.385	0.58576	0.0	0.278	1.60
	C _{COM}	0.375	0.43932	0.0	0.274	1.33
H ₂ ^{S9}	H	0.266	0.125	0.325	0.231	0.425
	H _{COM}	0.0	0.0	-0.65	0.0	0.0
CO ₂ ^{S10}	C	0.2757	0.2339	0.6512	0.235	0.614
	O	0.3033	0.6693	-0.3256	0.246	1.20
NH ₃ ^{S11}	N	0.342	0.711	-1.02	0.262	1.478
	H	0.0	0.0	0.34	0.0	0.0
H ₂ S ^{S8}	S	0.37	1.046	-0.47	0.272	2.018
	H	0.0	0.0	0.235	0.0	0.0

Supporting References

S1. J. VandeVondele, M. Krack, F. Mohamed, M. Parrinello, T. Chassaing, and J. Hutter, *Comput. Phys. Commun.* 2005, **167**, 103.

S2. S. Goedecker, M. Teter, and J. Hutter, *Phys. Rev. B* 1996, **54**, 1703.

S3. C. Hartwigsen, S. Goedecker, and J. Hutter, *Phys. Rev. B* 1998, **58**, 3641.

S4. A. D. Boese, N. L. Doltsinis, N. C. Handy, and M. Sprik, *J. Chem. Phys.* 1998, **112**, 1670.

- S5. J. Bai and X. C. Zeng, *Proc. Natl. Acad. Sci. U.S.A.* 2012, **109**, 21240.
- S6. P. Kumar, S. V. Buldyrev, F. W. Starr, N. Giovambattista, and H. E. Stanley, *Phys. Rev. E* 2005, **72**, 051503.
- S7. S. H. Han, M. Y. Choi, P. Kumar, and H. E. Stanley, *Nat. Phys.* 2010, **6**, 685.
- S8. G. A. Kaminski, R. A. Friesner, J. Tirado-Rives, and W. L. Jorgensen, *J. Phys. Chem. B* 2001, **105**, 6474.
- S9. S. Figueroa-Gerstenmaier, S. Giudice, L. Cavallo, and G. Milano, *Phys. Chem. Chem. Phys.*, 2009, **11**, 3935.
- S10. J. G. Harris and K. H. Yung, *J. Phys. Chem.* 1995, **99**, 12021.
- S11. R. C. Rizzo and W. L. Jorgensen, *J. Am. Chem. Soc.* 1999, **121**, 4827.